**Associazione Italiana
di Meccanica Teorica e Applicata**

AIMETA 2007

**Atti del XVIII Congresso dell'Associazione Italiana
di Meccanica Teorica e Applicata**

Brescia, 11-14 settembre 2007

a cura di

Angelo Carini
Giovanni Mimmi
Renzo Piva

Titolo: AIMETA 2007 - XVIII Congresso dell'Associazione Italiana di Meccanica Teorica e Applicata

An enhanced beam model of the mixed-mode bending (MMB) test

Stefano Bennati, Paolo Fisicaro, Paolo Sebastiano Valvo
Department of Structural Engineering, University of Pisa, Italy
E-mail: *s.bennati@ing.unipi.it, paolo.fisicaro@ing.unipi.it, p.valvo@ing.unipi.it*

Keywords: composite laminates, mixed mode delamination, mixed-mode bending test, elastic interface.

SUMMARY: The paper presents an enhanced model of the mixed-mode bending (MMB) test, commonly used for assessing the mixed-mode interlaminar fracture toughness of composite laminates. The specimen is considered as an assemblage of two identical sublaminates, partly bonded together by an elastic interface. Each sublaminate is modelled as an orthotropic beam, deformable due to bending, extension and shear. The interface is thought of as a continuous distribution of normal and tangential springs, whose elastic reactions produce transverse and axial loads in the sublaminates, as well as distributed couples. The mechanical behaviour of the system is described by a set of eighteen differential equations, endowed with suitable boundary conditions. The problem is split into the superposition of two subproblems, where the applied loads are symmetric and antisymmetric with respect to the interface plane, respectively. This approach allows for a simpler analytical solution and leads to a natural separation of the fracture modes within the context of beam theory. Through lengthy yet elementary calculations, a complete explicit solution to the original problem is deduced, in terms of displacements, internal forces and interfacial stresses. In particular, the mode I and II contributions to the energy release rate and the mode mixity ratio are determined.

1   INTRODUCTION

The separation between the laminae that make up a fibre-reinforced composite laminate, commonly known as delamination, is a major failure mode for this class of materials. Similar decohesion phenomena are observed in thin films, glued joints, sandwich panels, laminated wood, layered glass, and other layered materials in all fields of technology. A huge literature is available on this subject (for a first review, see [Garg, 1988; Sela and Ishai, 1989; Tay, 2003]).

The phenomenon of delamination can be analysed within the framework of Fracture Mechanics, where a delamination is properly regarded as an interlaminar fracture [Friedrich, 1989]. Under general service conditions, the growth of an interlaminar fracture in a composite laminate involves simultaneously the three modes of crack propagation: opening (I), sliding (II), and tearing (III). Experimental evidence shows that fracture toughness strongly depends on which propagation mode is active, or prevailing. Therefore, specific laboratory tests have been developed for assessing interlaminar toughness in each fracture mode [Adams *et al.*, 2003]. The double cantilever beam (DCB) test is the standard test for pure mode I, while the end notched flexure (ENF) test is commonly used for pure mode II. Also many mixed-mode tests have been proposed, where the delamination propagates under a (prescribed) mix of the modes I and II. Amongst the latter, the mixed-mode bending (MMB) test, introduced by Reeder and Crews [Reeder and Crews, 1990], is probably the most widely used one, and has recently become a standard in the USA [ASTM, 2006].

The MMB test is basically a bending test carried out on a (unidirectional) laminated specimen endowed at one of its ends with a pre-implanted delamination, splitting the specimen into two sublaminates of equal thickness (fig. 1). The specimen is loaded through a rigid lever, which divides the applied load, P, between a downward load, P_d, and an upward load, P_u. The length of the lever arm, c, can be adjusted in order to vary the ratio P_u / P_d and, consequently, the ratio between the fracture modes I and II. Within the context of *Simple Beam Theory* (SBT), the MMB test can be modelled through the superposition of the models developed for the DCB and ENF tests, separately. In particular, the energy release rate, G, can be obtained as the sum of a mode I contribution, G_I, corresponding to the DCB, and a mode II contribution, G_{II}, corresponding to the ENF. However, the SBT model suffers from some oversimplifying assumptions that lead to a poor matching with experimental results. A better description is obtained by the *Timoshenko Beam Theory* (TBT) model, which accounts also for shear deformability, or by more complex models [Kinloch *et al.*, 1993; Allix and Corigliano, 1996; Massabò and Cox, 2001; Szekrényes and Uj, 2006].
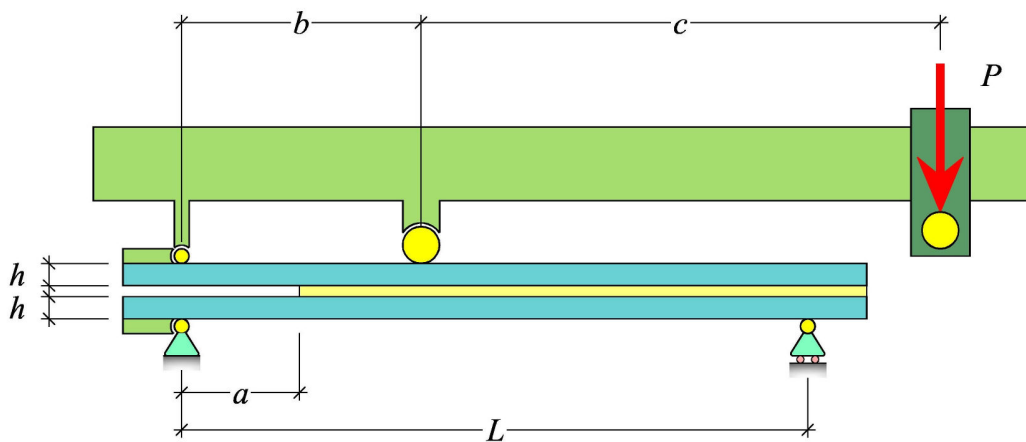
Figure 1 – The mixed-mode bending test.

This paper presents an *Enhanced Beam Model* (EBM) of the MMB test, where the laminated specimen is considered as an assemblage of two sublaminates, of equal thickness, partly bonded together by an interlaminar interface. This approach generalises an idea by [Kanninen, 1973], developed later by many Authors [Allix and Ladevèze, 1992; Corigliano, 1993; Point and Sacco, 1996; Bruno and Greco, 2001]. Although the model is based on a beam theory approach, a number of significant enhancements are introduced. Each sublaminate is modelled as a flexible orthotropic beam. Moreover, the deformations due to both shear and axial forces are taken into account. The interface is thought of as a continuous distribution of linear elastic springs, acting in both the normal and tangential directions with respect to the interface plane. The elastic reactions are proportional to the relative displacements between the points located at the bottom surface of the upper sublaminate and the upper

surface of the lower sublaminate. These reactions correspond to the normal and tangential interlaminar stresses, σ_z and τ_{zx}, which produce transverse and axial distributed loads on the sublaminates, respectively. Moreover, since there is an offset between the interface plane and the axes of the sublaminates, the tangential stresses produce also distributed couples, which are properly considered in the model.

The mechanical behaviour of the system is described by a set of eighteen differential equations, endowed with suitable boundary conditions. In order to simplify the analytical solution, the problem is split into the superposition of two subproblems corresponding to the symmetric and antisymmetric parts of the applied loads, respectively. Since the two sublaminates are identical in geometry and mechanical properties, it can be shown that in the symmetric problem the tangential interlaminar stresses vanish and so do the normal interlaminar stresses in the antisymmetric problem. Thus, this superposition scheme leads to the separation of fracture modes I and II. It is noteworthy that this result is obtained here within the natural context of the model (i.e. Beam Theory), without a somehow artificial exploitation of results coming from different theoretical settings [Wang and Qiao, 2006], such as Elasticity Theory [Suo and Hutchinson, 1990]. Finally, through lengthy but elementary calculations, whose details can be found in a forthcoming paper [Bennati *et al.*], a complete explicit solution to the stated differential problem is deduced. The analytic expressions of the displacement components, internal forces and interfacial stresses are obtained. In particular, the mode I and II contributions to the energy release rate and mode mixity are determined. Finally, useful correction factors, to be applied to the SBT expressions, are obtained.
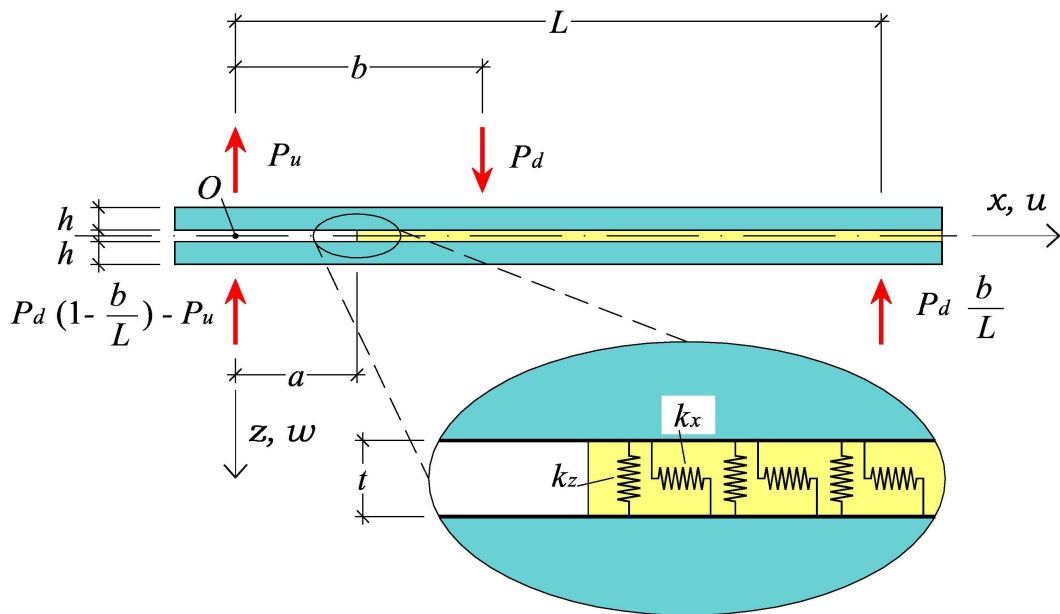
Figure 2 – The enhanced beam model of the MMB test, with a detail of the elastic interface.

3

2 THE MODEL

2.1 Formulation of the problem

The model is schematically represented in figure 2. A rectangular coordinate system $Oxyz$ is fixed with the origin O at the delaminated end of the specimen, the x-axis parallel to its axial direction and the z-axis pointing downwards. Let L, B, and $2h$ be the length, the width and the thickness of the specimen, respectively; let a be the delamination length. Let u_i and w_i denote the mid-plane displacements of the sublaminates along the x and z-axes, respectively, and let ϕ_i be the (counter-clockwise) cross-sectional rotations (the subscript i assumes the values 1 or 2 to refer, respectively, to the upper and lower sublaminates). Let E_x, E_y and G_{xy} be the elasticity moduli of the laminate in its material reference, whose axes are parallel to the fixed reference. Hence, let $\mathsf{A}_i = \mathsf{E}_x h = \mathsf{A}/2$, $\mathsf{C}_i = 5\mathsf{G}_{xy}h/6 = \mathsf{C}/2$, and $\mathsf{D}_i = \mathsf{E}_x h^3/12 = \mathsf{D}/8$ be, respectively, the extensional, shearing and bending stiffnesses of the sublaminates. These are related to the corresponding properties of the integer laminate, A, C, and D. On the upper sublaminate, an upward load, P_u, acts at the abscissa $x = 0$, and a downward load, P_d, acts at the abscissa $x = b$ (normally, $b = L/2$). The lower sublaminate is simply supported at its ends.

The equilibrium equations for the two sublaminates are

$$\frac{dN_i}{dx} + n_i = 0, \quad \frac{dQ_i}{dx} + q_i = 0, \quad \frac{dM_i}{dx} + m_i - Q_i = 0, \qquad i = 1, 2, \tag{1}$$

where N_i, Q_i, and M_i are, respectively, the axial force, the shear force and the bending moment, and

$$n_1 = -n_2 = \begin{cases} 0, & x \in [0, a[\\ B\tau_{zx}, & x \in [a, L] \end{cases}, \quad q_1 = -q_2 = \begin{cases} 0, & x \in [0, a[\\ B\sigma_z, & x \in [a, L] \end{cases}, \quad m_1 = m_2 = \begin{cases} 0, & x \in [0, a[\\ B\dfrac{h}{2}\tau_{zx}, & x \in [a, L] \end{cases} \tag{2}$$

are the corresponding distributed loads, related to the tangential and normal interfacial stresses,

$$\tau_{zx} = k_x\,\Delta u, \quad \sigma_z = k_z\,\Delta w, \tag{3}$$

which, in turn, through the elastic constants, k_x and k_z, are proportional to the axial and transverse relative displacements at the interface (of thickness $t \ll h$),

$$\Delta u = u_2 - u_1 - \frac{h}{2}(\phi_1 + \phi_2), \quad \Delta w = w_2 - w_1, \tag{4}$$

evaluated between the bottom and top surface of the upper and lower sublaminates, respectively.

The constitutive laws for the sublaminates can be written as follows

$$N_i = B\,\mathsf{A}_i\varepsilon_i, \quad Q_i = B\,\mathsf{C}_i\gamma_i, \quad M_i = B\,\mathsf{D}_i\kappa_i, \qquad i = 1, 2, \tag{5}$$

where

$$\varepsilon_i = \frac{du_i}{dx}, \quad \gamma_i = \phi_i + \frac{dw_i}{dx}, \quad \kappa_i = \frac{d\phi_i}{dx}, \qquad i = 1, 2, \tag{6}$$

are, respectively, the axial strain, the shear angle and the curvature of the sublaminates.

By introducing eqns. (2) through (6) in (1), after some simplifications, here omitted for the sake of brevity, we obtain the set of differential equations that govern the problem,

$$\frac{d^2 u_i}{dx^2} = 0, \quad \frac{d^2 w_i}{dx^2} + \frac{d\phi_i}{dx} = 0, \quad \frac{d^2 \phi_i}{dx^2} - \frac{4\mathsf{C}}{\mathsf{D}}(\phi_i + \frac{dw_i}{dx}) = 0, \qquad i = 1, 2, \tag{7a}$$

for $x \in [0, a]$, and

$$\frac{d^2 u_1}{dx^2} + \frac{d^2 u_2}{dx^2} = 0,$$

$$\frac{d^2 u_2}{dx^2} - \frac{d^2 u_1}{dx^2} - \frac{4k_x}{\mathsf{A}}[u_2 - u_1 - \frac{h}{2}(\phi_1 + \phi_2)] = 0,$$

$$\frac{d\phi_1}{dx} + \frac{d\phi_2}{dx} + \frac{d^2 w_1}{dx^2} + \frac{d^2 w_2}{dx^2} = 0,$$

$$\frac{d\phi_2}{dx} - \frac{d\phi_1}{dx} + \frac{d^2 w_2}{dx^2} - \frac{d^2 w_1}{dx^2} - \frac{4k_z}{\mathsf{C}}(w_2 - w_1) = 0, \tag{7b}$$

$$\frac{d^2 \phi_1}{dx^2} + \frac{d^2 \phi_2}{dx^2} - \frac{4\mathsf{C}}{\mathsf{D}}(\phi_1 + \phi_2 + \frac{dw_1}{dx} + \frac{dw_2}{dx}) + \frac{2\mathsf{A}h}{\mathsf{D}}(\frac{d^2 u_2}{dx^2} - \frac{d^2 u_1}{dx^2}) = 0,$$

$$\frac{d^2 \phi_2}{dx^2} - \frac{d^2 \phi_1}{dx^2} - \frac{4\mathsf{C}}{\mathsf{D}}(\phi_2 - \phi_1 + \frac{dw_2}{dx} - \frac{dw_1}{dx}) = 0,$$

for $x \in [a, b]$ and $x \in [b, L]$. The differential problem is completed by boundary conditions describing the restraints at $x = 0$ and $x = L$, as well as the (dis)continuity of the solution at $x = a$ and $x = b$. Their expressions are here omitted for the sake of brevity (see [Bennati *et al.*]).

2.2 Solution strategy and fracture mode separation

The differential problem to be solved, in terms of the generalised displacements, is composed by 18 equations: eqns. (7a) are in number of 3 (for the upper sublaminate) + 3 (for the lower sublaminate); eqns. (7b) are in number of 6 (for $x \in [a, b]$) + 6 (for $x \in [b, L]$). The solution of eqns. (7a) is straightforward; instead, the solution of eqns. (7b) is more involved. In what follows only a sketch of the solution strategy is presented, and the details are postponed to a forthcoming paper [Bennati *et al.*].
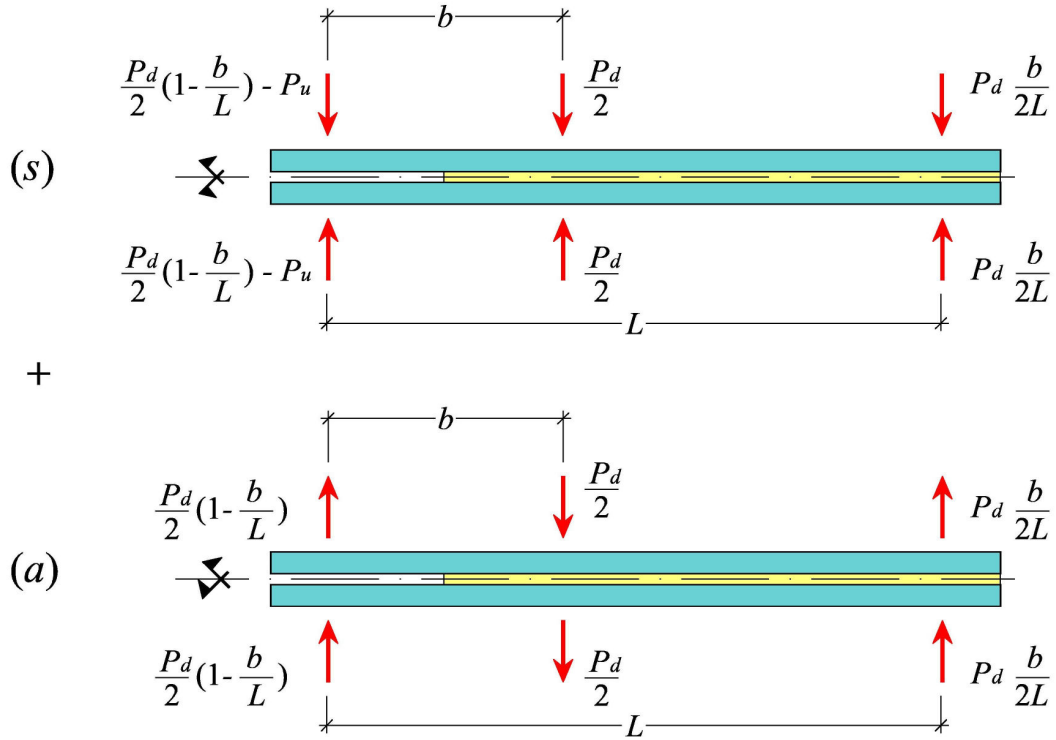
Figure 3 – Symmetric and antisymmetric load systems.

In order to simplify the solution of eqns. (7b), it is convenient to split the original problem into the sum of two subproblems, (*s*) and (*a*), where the symmetric and antisymmetric parts of the loads are applied, respectively (fig. 3). Thus, the sought solution can be expressed as

$$u_i = u_i^{(s)} + u_i^{(a)}, \quad w_i = w_i^{(s)} + w_i^{(a)}, \quad \phi_i = \phi_i^{(s)} + \phi_i^{(a)}, \qquad i = 1, 2. \tag{8}$$

Since the two sublaminates are identical, as far as geometry and mechanical properties are concerned, the solutions must satisfy the same (anti)symmetries, namely

$$u_1^{(s)} = u_2^{(s)}, \quad w_1^{(s)} = -w_2^{(s)}, \quad \phi_1^{(s)} = -\phi_2^{(s)}, \tag{9a}$$

and

$$u_1^{(a)} = -u_2^{(a)}, \quad w_1^{(a)} = w_2^{(a)}, \quad \phi_1^{(a)} = \phi_2^{(a)}. \tag{9b}$$

6

By substituting eqns. (8) and (9) into (3) and (4), it is immediately seen that

$$\Delta u^{(s)} = 0 \Rightarrow \tau_{zx}{}^{(s)} = 0, \quad \text{and} \quad \Delta w^{(a)} = 0 \Rightarrow \sigma_z{}^{(a)} = 0. \tag{10}$$

It is thus demonstrated that the symmetric load system only produces normal interfacial stresses, so it is related to pure mode I fracture (opening); conversely, the antisymmetric load system is responsible only for tangential interfacial stresses, so it corresponds to pure mode II fracture (sliding).

2.3 Explicit expressions of the solution

The explicit expressions for the generalised displacements, as well as for the internal forces in the upper and lower sublaminates have been obtained [Bennati *et al.*].

In particular, the normal and tangential interlaminar stresses at the elastic interface are

$$\sigma_z = \begin{cases} k_z[\beta_1 \cosh \lambda_1(x-a) + \beta_2 \sinh \lambda_1(x-a) + \beta_3 \cosh \lambda_2(x-a) + \beta_4 \sinh \lambda_2(x-a)], & x \in [a, b[\\[2mm] k_z[\beta_1 \cosh \lambda_1(x-a) + \beta_2 \sinh \lambda_1(x-a) + \beta_3 \cosh \lambda_2(x-a) + \beta_4 \sinh \lambda_2(x-a)] + \\[2mm] \quad + \dfrac{P_d}{2B} \dfrac{\lambda_1^3 \sinh \lambda_1(x-b) - \lambda_2^3 \cosh \lambda_1(x-b)}{\lambda_1^2 - \lambda_2^2}, & x \in [b, L] \end{cases}$$

$$\tau_{zx} = \begin{cases} \dfrac{P_d}{B} \dfrac{Ah}{D+Ah^2} \{(1-\dfrac{b}{L})[1 + \lambda_5\, a\dfrac{\cosh \lambda_5(L-x)}{\sinh \lambda_5(L-a)}] - \dfrac{\sinh \lambda_5(L-b)}{\sinh \lambda_5(L-a)} \cosh \lambda_5(L-x)\}, & x \in [a, b[\\[4mm] -\dfrac{P_d}{B} \dfrac{Ah}{D+Ah^2} \{\dfrac{b}{L} - [\lambda_5\, a(1-\dfrac{b}{L}) + \sinh \lambda_5(b-a)]\dfrac{\cosh \lambda_5(L-x)}{\sinh \lambda_5(L-a)}\}, & x \in [b, L] \end{cases}$$

$$\tag{11}$$

where

$$\lambda_1 = \sqrt{\frac{2k_z}{C}(1 + \sqrt{1 - \frac{4C^2}{k_z D}})}, \quad \lambda_2 = \sqrt{\frac{2k_z}{C}(1 - \sqrt{1 - \frac{4C^2}{k_z D}})}, \quad \lambda_5 = 2\sqrt{k_x(\frac{1}{A} + \frac{h^2}{D})} \tag{12}$$

are constants related to the roots of the characteristic equations of the differential equations (7b), and β_1, β_2, β_3, and β_4 are constants depending on the loads, P_u and P_d. Their explicit expressions, obtained by imposing the boundary conditions, are rather lengthy and can be found in [Bennati *et al.*].

Due to the presence of the elastic interface, the modal contributions to the energy release rate are

$$G_I = \frac{1}{2} k_z [\Delta w(a)]^2, \qquad G_{II} = \frac{1}{2} k_x [\Delta u(a)]^2. \tag{13}$$

or, more concisely,

$$G_I = \mu_I G_I^{SBT}, \qquad G_{II} = \mu_{II} G_{II}^{SBT}, \tag{14}$$

where

$$G_I^{SBT} = \frac{8 P_I^2 a^2}{B^2 \mathsf{D}}, \qquad G_{II}^{SBT} = \frac{3 P_{II}^2 a^2}{8 B^2 \mathsf{D}}, \tag{15}$$

are the mode I and II energy release rates, computed according to the Simple Beam Theory (where fracture mode separation is obtained by letting $P_I = P_u - (1 - b/L) P_d / 2$ and $P_{II} = 2(1 - b/L) P_d$), and

$$\mu_I = [1 + \frac{(\lambda_1 + \lambda_2)^2 (1 - 1/C_1 C_2 - T_1 T_2) + (\lambda_1^2 - \lambda_2^2)(\lambda_1 T_2 - \lambda_2 T_1)/\lambda_1 \lambda_2 a}{(\lambda_1^2 + \lambda_2^2) T_1 T_2 - 2\lambda_1 \lambda_2 (1 - 1/C_1 C_2)}]^2,$$

$$\mu_{II} = \{\coth \lambda_5 (L - a) + \frac{1}{\lambda_5 a}[1 - \frac{1}{1 - b/L} \frac{\sinh \lambda_5 (L - b)}{\sinh \lambda_5 (L - a)}]\}^2, \tag{16}$$

are modal correction factors. In (16) we have set $C_j = \cosh \lambda_j (L - a)$, $T_j = \tanh \lambda_j (L - a)$, $j = 1, 2$.

3   APPLICATION

For the sake of illustration, we consider the case of a 24-ply graphite/PEEK unidirectional laminate having the following geometric and mechanic properties [Reeder and Crews, 1990]

L = 100 mm, B = 25 mm, $2h$ = 3.1 mm,
E_x = 116000 N/mm^2, $\mathsf{E}_y = \mathsf{E}_z$ = 10100 N/mm^2, $\mathsf{G}_{xy} = \mathsf{G}_{zx}$ = 5500 N/mm^2.

The delamination length, a, ranges from 25 to 45 mm. The applied load is $P = 100\,\text{N}$. The downward load is placed at the mid-span, so $b = L/2$. The lever arm, c, is 44 mm, which, according to the Simple Beam Theory, corresponds to a mode mixity ratio, $\Psi = G_I^{SBT} / G_{II}^{SBT} = 1$.

Figures 4a and 4b show the mode I and II energy release rates, G_I and G_{II}, as functions of the delamination length, a. Here and in the following, the (red) dashed curves refer to the Simple Beam Theory model (SBT), the (black) dash-dot curves to the Timoshenko Beam Theory model (TBT) and the (blue) continuous curves refer to our Enhanced Beam Model (EBM). Three orders of magnitude for the elastic interface constants, k_x and k_z, are used: 10^3, 10^4, and 10^5 N/mm^3.

With reference to figure 4a, we notice that the SBT and TBT models predict nearly coincident values for the mode I energy release rate, G_I^{SBT} and G_I^{TBT}. Instead, the values predicted by our model appear to be quite higher. The difference between the G_I of the EBM and G_I^{SBT} diminishes as the normal elastic constant, k_z, increases. It is noteworthy that, for k_z approaching infinity, the predictions of the EBM reach a limit value which is different from the simpler models. This is a consequence of the

higher deformability of the proposed model with respect to models where the integer part of the specimen is modelled as a monolithic beam. Actually, it can be shown that, since we consider the shear deformability of beams, even in the limit case of a rigid interface, the upper and lower sublaminates maintain the possibility of different cross-sectional rotations under symmetric (mode I) load conditions. This is not the case when antisymmetric (mode II) load conditions are considered (fig. 4b). As the tangential elastic constant, k_x, approaches infinity, the G_{II} of the EBM tends towards G_{II}^{SBT}. A careful reader would surely notice that the curve representing the TBT is missing from the plot of the mode II energy release rate. This is not a misprint! Though different statements can be found in the literature, for mode II, the TBT yields identical predictions to the SBT. In fact, the shear deformability of the beams should not influence the mode II fracture propagation (for a deeper discussion see [Valvo]).

a)   b)
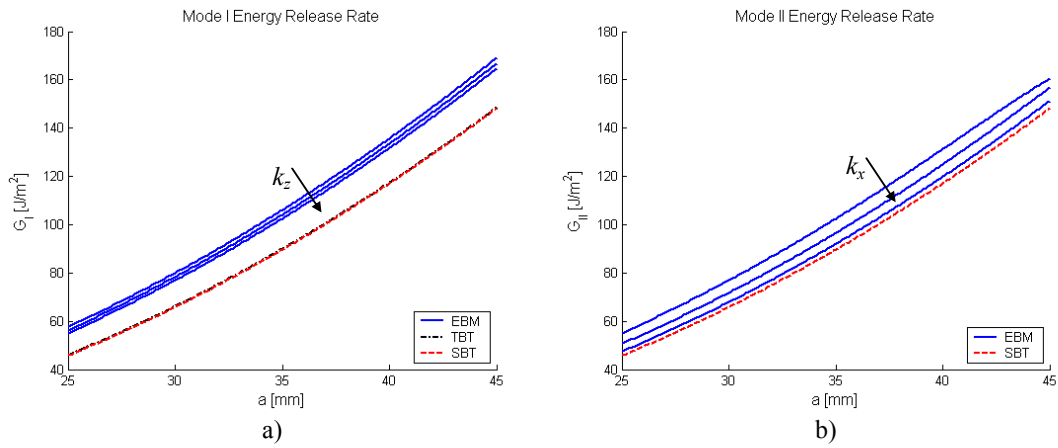
Figure 4 – Mode I (a) and Mode II (b) energy release rates vs. delamination length.

a)   b)
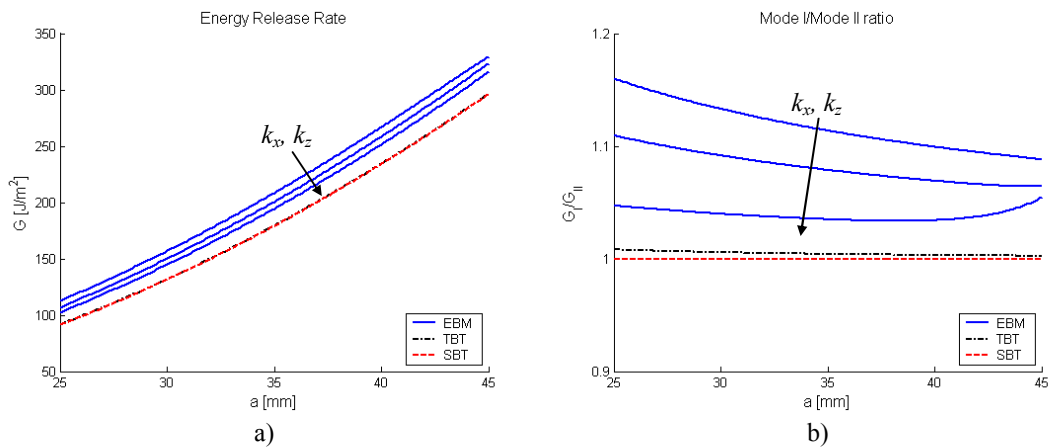
Figure 5 – Energy release rate (a) and Mode I/II energy release rate ratio (b) vs. delamination length.

Figure 5a shows the total energy release rate, $G = G_I + G_{II}$, as a function of the delamination length, a. As the elastic constants, k_z and k_x, increase, the energy release rate gets closer to the curves representing the SBT and TBT models. The limit value in the case of a rigid interface, however, is greater than the predictions of the simpler models, because of the influence of the shear deformability on the G_I contribution.

Figure 5b represents the mode mixity ratio, G_I / G_{II}, as a function of the delamination length, a. Differing from the SBT, the EBM yields a non-constant mode mixity ratio and shows a significant scatter also with reference to the TBT. The difference with the simpler models becomes smaller as the elastic constants increase.

Figure 6a and 6b show in semi-logarithmic scale the mode I and II correction factors, μ_I and μ_{II}, as functions of the elastic constants, k_z and k_x, respectively. In both cases, as the elastic constant goes to infinity, the curves reach a horizontal asymptote. For mode II, the limit value of the correction factor is one (fig. 6b); for mode I, the limit value depends on the shear stiffness, C, and approaches unity only when also the shear stiffness tends to infinity (fig. 6a).

a)   b)
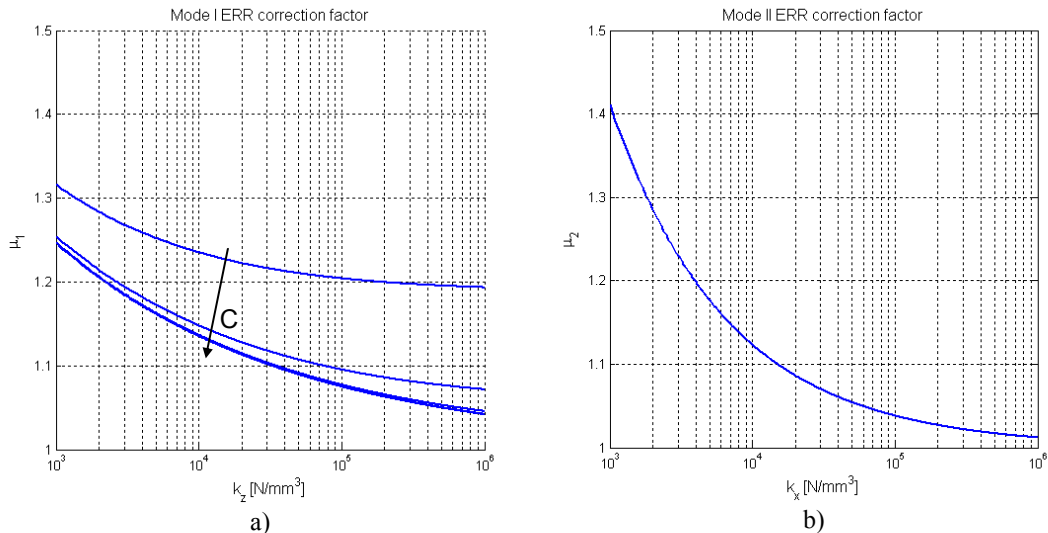
Figure 6 – Mode I (a) and Mode II (b) correction factors vs. elastic constants.

4   CONCLUSIONS

An enhanced beam model of the mixed-mode bending test has been developed. The main improvement with respect to other models available in the literature stems from the introduction of an elastic interface, which produces distributed loads and couples on the sublaminates. These ones have been modelled as elastic beams, taking into account the bending, axial and shear deformability. A complete analytical solution has been determined, in particular for the interlaminar stresses and the mode I and II contributions to the energy release rate.

The example shown above has highlighted a significant dependence of the predictions of the EBM on the values of the interfacial elastic constants. As a first attempt, we can define these ones as

$$k_x = \frac{G_{zx}}{t_x}, \qquad k_z = \frac{E_z}{t_z}, \qquad (17)$$

where t_x and t_z are characteristic lengths, depending on the thickness of the sublaminates, related to the size of the fracture process zone.
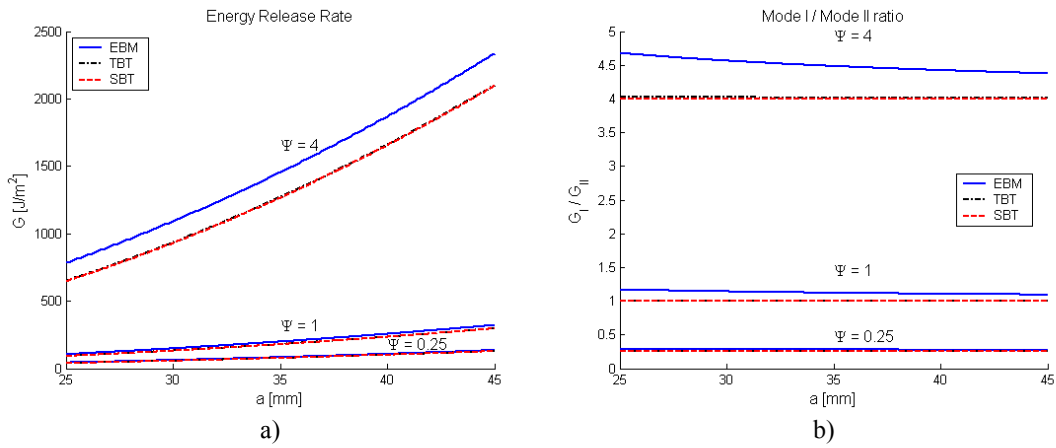
Figure 7 – Energy release rate vs. delamination length for various mode mixity ratios.

Figures 7a and 7b are obtained by setting $t_x = h \, / \, 10$, and $t_z = h$. The plots show the total energy release rate, G, and the mode mixity ratio, $G_I \, / \, G_{II}$, as functions of the delamination length, a. Three values of the lever arm, c, are used: 28, 44 and 108 mm. According to the Simple Beam Theory, the corresponding ratios, $\Psi = G_I^{SBT} \, / \, G_{II}^{SBT}$, are 1/4, 1/1, and 4/1, respectively.

As a concluding remark, we observe that the values of the interfacial elastic constants could be assigned in order to match the experimental results or the predictions of numerical models of the MMB test. Nevertheless, if the proposed model is supposed to furnish a prediction of the MMB test results, and not only an *a posteriori* description of these ones, the values of the constants should be fixed according to a micro/meso-mechanical model, supported by *ad hoc* experimental tests. The matter is surely worth further investigation.

References:
Adams, D.F., Carlsson, L.A. and Byron Pipes, R. (2003). *Experimental Characterization of Advanced Composite Materials – 3rd edition*. CRC Press, Boca Raton.
Allix, O. and Ladevèze, P. (1992). Interlaminar interface modelling for the prediction of delamination, *Compos. Struct.*, 22:235-242.

Allix, O. and Corigliano, A. (1996). Modeling and simulation of crack propagation in mixed-modes interlaminar fracture specimens, *Int. J. Fract.*, 77:111-140.

ASTM (2006). *ASTM Standard D6671/D6671M-06, Standard Test Method for Mixed Mode I-Mode II Interlaminar Fracture Toughness of Unidirectional Fiber Reinforced Polymer Matrix Composites*, American Society for Testing and Materials, West Conshohocken, PA.

Bennati, S., Fisicaro, P. and Valvo P.S. An enhanced beam model of the general mixed-mode bending (MMB) test for composite materials, *Meccanica* (to be submitted).

Bruno, D. and Greco, F. (2001). Mixed mode delamination in plates: a refined approach, *Int. J. Solids Struct,*, 38:9149-9177.

Corigliano, A. (1993). Formulation, identification and use of interface models in the numerical analysis of composite delamination, *Int. J. Solids Struct,*, 30:2779-2811.

Friedrich, K., editor (1989). *Application of Fracture Mechanics to Composite Materials*. Elsevier, Amsterdam.

Garg, A.C. (1988). Delamination – A damage mode in composite structures, *Eng. Fract. Mech.*, 29:557-584.

Kanninen, M.F. (1973). An augmented double cantilever beam model for studying crack propagation and arrest, *Int. J. Fract.*, 9:83-92.

Kinloch, A. J., Wang, Y., Williams, J.G. and Yayla P. (1993). The mixed-mode delamination of fibre composite materials, *Comp. Sci. Tech.*, 47:225-237.

Massabò, R. and Cox, B.N. (2001). Unusual characteristics of Mixed-Mode Delamination Fracture in the Presence of Large-Scale Bridging, *Mech. Compos. Mat. Struct.*, 8:61-80.

Reeder, J.R. and Crews, J.H. Jr. (1990). Mixed-mode bending method for delamination testing, *AIAA Journal*, 28:1270-1276.

Point, N. and Sacco, E. (1996). A delamination model for laminated composites, *Int. J. Solids Struct.*, 33:483-509.

Sela, N. and Ishai, O. (1989). Interlaminar fracture toughness and toughening of laminated composite materials: A review, *Composites*, 20:423-435.

Szekrényes, A. and Uj, J. (2006). Comparison of some improved solutions for mixed-mode composite delamination coupons, *Compos. Struct.*, 72:321-329.

Suo, Z. and Hutchinson, J.W. (1990). Interface crack between two elastic layers, *Int. J. Fract.*, 43:1-18.

Tay, T.E. (2003). Characterization and analysis of delamination fracture in composites: An overview of developments from 1990 to 2001, *Appl. Mech. Rev.*, 56:1-31.

Valvo, P.S. Does shear deformability influence the mode II fracture of delaminated beams?, *Int. J. Fract.* (to be submitted).

Wang, J. and Qiao, P. (2006). Fracture Analysis of Shear Deformable Bi-Material Interface, *ASCE J. Eng. Mech.*, 132:306-316.